JACS
JOURNAL OF THE AMERICAN CHEMICAL SOCIETY
Communication
pubs.acs.org/JACS

A Luminescent Mixed-Lanthanide Metal–Organic Framework Thermometer

Yuanjing Cui,[†,‡] Hui Xu,[†] Yanfeng Yue,[‡] Zhiyong Guo,[‡] Jiancan Yu,[†] Zhenxia Chen,[§] Junkuo Gao,[†] Yu Yang,[†] Guodong Qian,*[,†] and Banglin Chen*[,‡]

[†]State Key Laboratory of Silicon Materials, Cyrus Tang Center for Sensor Materials and Applications, Department of Materials Science and Engineering, Zhejiang University, Hangzhou 310027, P. R. China

[‡]Department of Chemistry, University of Texas at San Antonio, San Antonio, Texas 78249-0698, United States

[§]Department of Chemistry, Fudan University, Shanghai 200433, P. R.China

Supporting Information

ABSTRACT: A luminescent mixed lanthanide metal–organic framework approach has been realized to explore luminescent thermometers. The targeted self-referencing luminescent thermometer **$Eu_{0.0069}Tb_{0.9931}$-DMBDC** (DMBDC = 2, 5-dimethoxy-1, 4-benzenedicarboxylate) based on two emissions of Tb^{3+} at 545 nm and Eu^{3+} at 613 nm is not only more robust, reliable, and instantaneous but also has higher sensitivity than the parent MOF **Tb-DMBDC** based on one emission at a wide range from 10 to 300 K.

Self-assembly of metal ions and organic linkers into luminescent metal–organic frameworks (MOFs) has provided the bright promise to develop functional luminescent MOF materials.[1−5] This is because both the inorganic and organic moieties can provide the platforms to generate luminescence, while metal–ligand charge-transfer related luminescence can add another dimensional luminescent functionality. Furthermore, some guest molecules within MOFs can also emit and/or induce luminescence. Compared with the traditional molecular approach, by making use of molecular organic and coordination compounds to explore functional luminescent materials, the MOF approach also has the advantage to collaboratively interplay/interact with each other among the periodically located luminescent centers to direct new functionalities. In fact, a variety of luminescent MOFs have been realized for their diverse applications on chemical sensing, light-emitting devices, and biomedicine over the past two decades.[6−24]

Temperature-dependent luminescence is a very common phenomenon which has been utilized to develop luminescent thermometers based on molecular coordination compounds and their nanoparticles.[25−32] Such new luminescent thermometers have distinct advantages over other conventional thermometers because of their fast response, high sensitivity, noninvasive operation, and inertness to strong electric or magnetic fields. However, most luminescent thermometers explored until now are only based on the temperature-dependent luminescence intensity of one transition whose accuracy can be heavily affected by the quantity of the luminophore, excitation power, and the drifts of the optoelectronic system; and/or on lifetime which requires a relatively long time and the computational treatment. Recently, Carlos has pioneered the two luminescent transitions approach based on molecular coordination compounds and nanoparticles to explore more robust and reliable luminescent thermometers.[28] To dope Eu^{3+} into an isostructural Tb^{3+}-MOF to form the mixed-lanthanide metal organic frameworks $(Eu_xTb_{1-x})_2(DMBDC)_3(H_2O)_4{\cdot}DMF{\cdot}H_2O$ (**Eu_xTb_{1-x}-DMBDC**; DMBDC = 2,5-dimethoxy-1,4-benzenedicarboxylate) in which the second luminescent transition from the $^5D_0 \rightarrow {}^7F_2$ of Eu^{3+} at 613 nm can be readily generated in addition to the original one of the Tb^{3+} at 545 nm from the $^5D_4 \rightarrow {}^7F_5$ transition, while their temperature-dependent luminescent intensity ratios I_{Tb}/I_{Eu} can be optimized by the controlled doping of different amounts of Eu^{3+}, herein we report the first luminescent mixed-lanthanide MOF thermometer **$Eu_{0.0069}Tb_{0.9931}$-DMBDC** at a wide temperature range.

Reacting H_2DMBDC with $Tb(NO_3)_3$ or $Eu(NO_3)_3$ via a solvothermal method in mixed solvents of dimethylformamide (DMF), ethanol, and water yielded colorless rodlike crystals of $Tb_2(DMBDC)_3(H_2O)_4{\cdot}DMF{\cdot}H_2O$ (**Tb-DMBDC**) or $Eu_2(DMBDC)_3(H_2O)_4{\cdot}DMF{\cdot}H_2O$ (**Eu-DMBDC**), respectively.

Single-crystal X-ray diffraction analyses indicate that the MOFs **Tb-DMBDC** and **Eu-DMBDC** are isostructural, exhibiting three-dimensional (3D) rod-packing structures as shown in Figure 1 for the **Tb-DMBDC** in which each Tb^{3+}-carboxylate infinite SBU is connected to other six chains through the phenylene portion of the DMBDC linkers. Accordingly, the Eu^{3+}/Tb^{3+} mixed lanthanide MOFs of the general formula $(Eu_xTb_{1-x})_2(DMBDC)_3(H_2O)_4{\cdot}DMF{\cdot}H_2O$ (**Eu_xTb_{1-x}-DMBDC**) (x = 0.0011, 0.0046, and 0.0069) can be readily synthesized by varying the original molar ratios of $Eu(NO_3)_3$ to $Tb(NO_3)_3$ through the same synthetic procedures. The molar ratios of Eu^{3+}/Tb^{3+} in the resulting mixed lanthanide MOFs match with the original molar ratios of Eu^{3+}/Tb^{3+} in the starting chemicals, which were exclusively confirmed by inductively coupled plasma spectroscopy (ICP). As expected, these mixed lanthanide MOFs are isostructural to

Received: November 28, 2011
Published: February 21, 2012

   dx.doi.org/10.1021/ja2108036 | J. Am. Chem. Soc. 2012, 134, 3979–3982

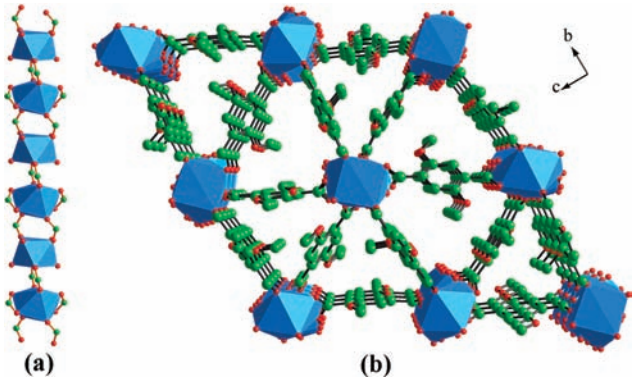

Figure 1. Crystal structure of **Tb-DMBDC** indicating (a) 1D Tb^{3+}-carboxylate chain as the infinite SBU and (b) the crystal packing viewed along the *a* crystallographic direction (Tb, blue polyhedra; C, green; O, red; H atoms are omitted for clarity).

the parent ones **Tb-DMBDC** and **Eu-DMBDC**, as shown in their powder X-ray diffraction patterns (Figure S1).

To determine whether the DMBDC linkers provide efficient sensitization for the lanthanide ions, the room temperature excitation and emission spectra of the MOFs were examined in the solid state. All the excitation spectra display an intense and broad band with a maximum at around 381 nm, which is attributed to the $\pi-\pi^*$ electron transition of DMBDC linkers (Figures S7–S11). Upon excitation at 381 nm, these MOFs exhibit the characteristic lanthanide luminescence with sharp and well-separated emission bands. **Tb-DMBDC** displays the emission peaks at 489, 545, 587, and 621 nm which can be assigned to the $^5D_4 \rightarrow {}^7F_J$ (J = 6, 5, 4, and 3) transitions of Tb^{3+} ions; while **Eu-DMBDC** exhibits emissions at 592, 613, 652, and 701 nm which are from the $^5D_0 \rightarrow {}^7F_J$ (J = 1, 2, 3, and 4) transitions of Eu^{3+} ions. As expected, all the doped mixed lanthanide MOFs **$Eu_{0.0011}Tb_{0.9989}$-DMBDC**, **$Eu_{0.0046}Tb_{0.9954}$-DMBDC**, and **$Eu_{0.0069}Tb_{0.9931}$-DMBDC** simultaneously show both the characteristic emissions of the Tb^{3+} and the Eu^{3+} ions. These results clearly indicate that the DMBDC is an excellent antenna chromophore for sensitizing both Tb^{3+} and Eu^{3+} ions. It needs to be particularly mentioned that the emission of the Eu^{3+} ions in mixed lanthanide MOFs are further sensitized by the Tb^{3+} ions within the same frameworks. Such Tb^{3+}-to-Eu^{3+} energy transfer behaviors have been confirmed by the emission spectra excited at 488 nm of the $^7F_6 \rightarrow {}^5D_4$ transition from the Tb^{3+} ions at room temperature (Figures S12–S14).

The temperature-dependent photoluminescent (PL) properties of the MOFs were investigated both in terms of intensity and lifetime in order to establish their potentials as luminescent thermometers. The temperature dependence of the emission spectra of **Tb-DMBDC**, **Eu-DMBDC** and **$Eu_{0.0069}Tb_{0.9931}$-DMBDC** from 10 to 300 K are illustrated in Figure 2a–c, and the integrated intensities of the $^5D_4 \rightarrow {}^7F_5$ (Tb^{3+}, 545 nm) and $^5D_0 \rightarrow {}^7F_2$ (Eu^{3+}, 613 nm) transitions are shown in Figure 2d. The luminescent intensity of both Tb^{3+} and Eu^{3+} in **Tb-DMBDC** and **Eu-DMBDC** decreases gradually as the temperature increases which is normal due to the thermal activation of nonradiative-decay pathways. However, the mixed lanthanide MOF **$Eu_{0.0069}Tb_{0.9931}$-DMBDC** exhibits a significantly different temperature-dependent luminescent behavior from those of **Tb-DMBDC** and **Eu-DMBDC**. The emission intensity of the Tb^{3+} ions in **$Eu_{0.0069}Tb_{0.9931}$-DMBDC** decreases, while that of the Eu^{3+} increases with the temperature. At 10 K, the emission bands of 613 (Eu^{3+}) and 545 (Tb^{3+}) nm have comparable intensity, whereas at 300 K, the emission of Eu^{3+} almost

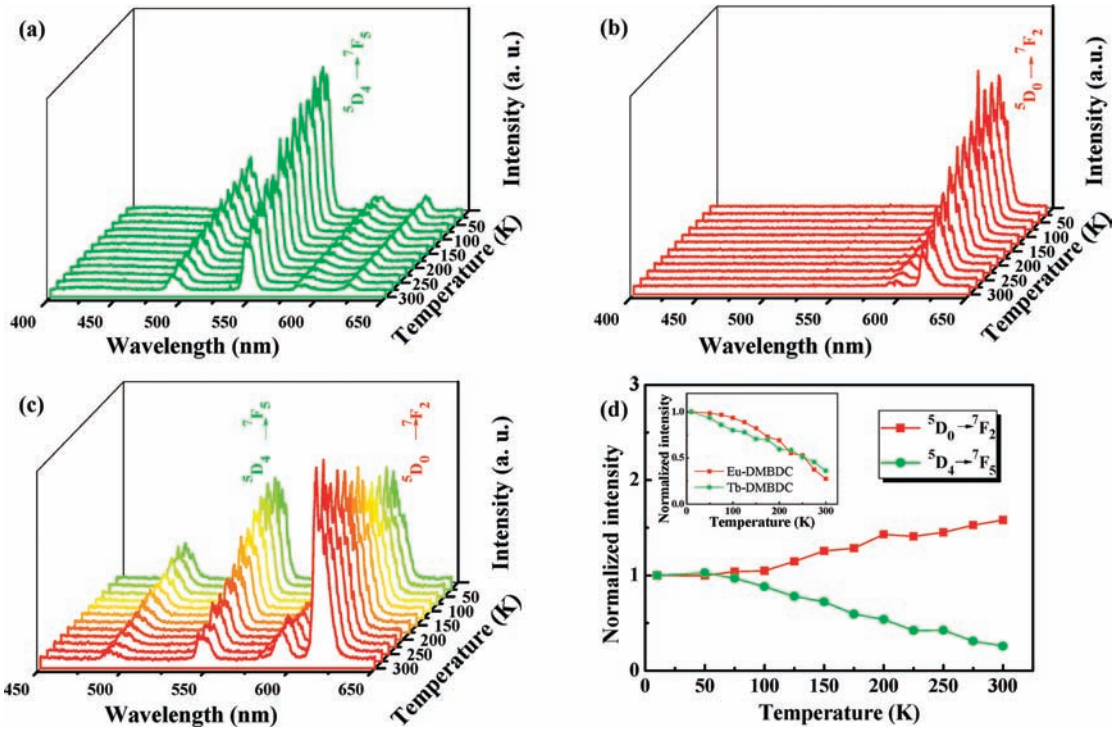

Figure 2. Emission spectra of (a) **Tb-DMBDC**, (b) **Eu-DMBDC**, (c) **$Eu_{0.0069}Tb_{0.9931}$-DMBDC** recorded between 10 and 300 K (excited at 355 nm from the third harmonic of a Nd:YAG laser), and (d) temperature dependence of integrated intensities of the $^5D_4 \rightarrow {}^7F_5$ (534–562 nm) and $^5D_0 \rightarrow {}^7F_2$ (605–633 nm) transitions for **$Eu_{0.0069}Tb_{0.9931}$-DMBDC**. (Inset) Temperature-dependent integrated intensity of the $^5D_4 \rightarrow {}^7F_5$ transition of **Tb-DMBDC** and $^5D_0 \rightarrow {}^7F_2$ transition of **Eu-DMBDC**.

dx.doi.org/10.1021/ja2108036 | *J. Am. Chem. Soc.* 2012, 134, 3979–3982

dominates the whole spectrum although the Eu^{3+} content in the **$Eu_{0.0069}Tb_{0.9931}$-DMBDC** is very low. Similar results were also observed in other mixed lanthanide MOFs (Figures S15−S18). Such temperature-dependent emission spectra are repeatable and reversible.

The different temperature-dependent luminescent emissions of $^5D_4 \rightarrow {}^7F_5$ (Tb^{3+}, 545 nm) and $^5D_0 \rightarrow {}^7F_2$ (Eu^{3+}, 613 nm) in the same mixed lanthanide MOFs have enabled them to be excellent candidates for self-referencing luminescent thermometers; we thus examined the **$Eu_{0.0069}Tb_{0.9931}$-DMBDC** in detail. As shown in Figure 3, the temperature can be readily correlated

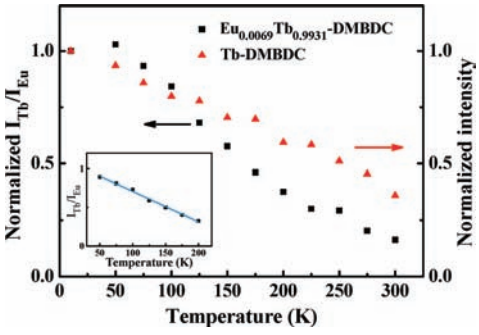

Figure 3. Temperature dependence of the integrated intensity ratio of Tb^{3+} (545 nm) to Eu^{3+} (613 nm) for **$Eu_{0.0069}Tb_{0.9931}$-DMBDC** (black squares), and temperature dependence of integrated intensity of Tb^{3+} (545 nm) for **Tb-DMBDC** (red triangles). (Inset) Fitted curves of the integrated intensity ratio for **$Eu_{0.0069}Tb_{0.9931}$-DMBDC** from 50 to 200 K.

to the emission intensity ratio of the $^5D_4 \rightarrow {}^7F_5$ (Tb^{3+}, 545 nm) to $^5D_0 \rightarrow {}^7F_2$ (Eu^{3+}, 613 nm) transition (I_{Tb}/I_{Eu}), which does not require any additional calibration of luminescence intensity. Such a mixed lanthanide MOF thermometer is not only more robust and reliable but also exhibits higher sensitivity than the **Tb-DMBDC** based on the single transition of $^5D_4 \rightarrow {}^7F_5$ at 545 nm, as demonstrated in its larger slope (Figure 3, black) than the temperature-dependent luminescence decay rate (Figure 3, red). The fact that the temperature can be linearly related to I_{Tb}/I_{Eu} by the eq 1 from 50 to 200 K

$$T = 287.09 - 263.85 I_{Tb}/I_{Eu} \quad (1)$$

indicates that **$Eu_{0.0069}Tb_{0.9931}$-DMBDC** is an excellent luminescent thermometer at this temperature range (Figure 3, inset). Such a luminescent thermometer at this temperature range has been rarely explored[27] although thermocouples and resistance thermometers based on platinum, germanium, or carbon have been available.

Because Tb^{3+} and Eu^{3+} within **$Eu_{0.0069}Tb_{0.9931}$-DMBDC** emit different colors of green at 545 nm and red at 613 nm, respectively; such a luminescent mixed lanthanide MOF thermometer has also allowed us to directly visualize the temperature change instantly and straightforwardly, another very unique feature for two emissions based luminescent thermometers. As shown in Figure 4, the temperature dependent luminescence colors of **$Eu_{0.0069}Tb_{0.9931}$-DMBDC** are systematically tuned from the green-yellow to red from 10 to 300 K, which can be clearly and directly observed even by the naked eye or camera. Based on Commission Internacionale d'Eclairage (CIE) chromaticity diagram, the corresponding CIE coordinates change from (0.428, 0.442) at 10 K to (0.575, 0.347) at 300 K.

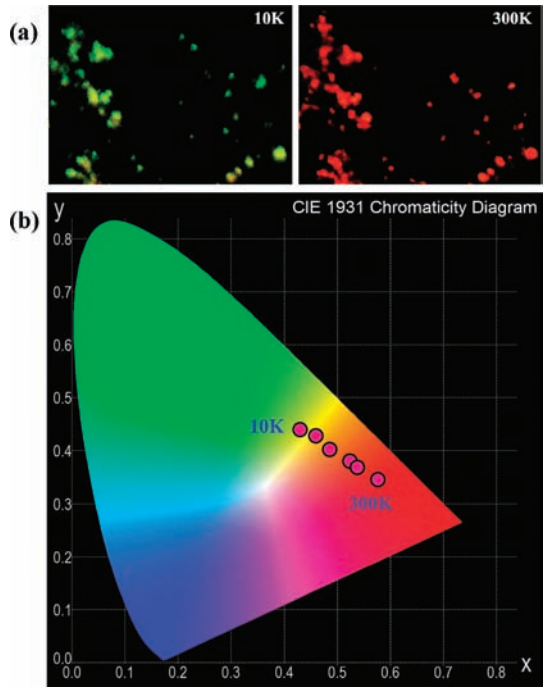

Figure 4. (a) Photograph of the luminescent **$Eu_{0.0069}Tb_{0.9931}$-DMBDC** at 10 K (left) and 300 K (right), excited at 312 nm. (b) CIE chromaticity diagram showing the luminescence color of $Eu_{0.0069}Tb_{0.9931}$-DMBDC at different temperatures.

The unique temperature-dependent emissions and luminescence colors in **$Eu_{0.0069}Tb_{0.9931}$-DMBDC** may be rationalized by the temperature-dependent energy transfer probability from the Tb^{3+} to Eu^{3+} ions. The variable temperature emission spectra of **$Eu_{0.0069}Tb_{0.9931}$-DMBDC** excited at 488 nm clearly demonstrates that the probability of the Tb^{3+}-to-Eu^{3+} energy transfer is significantly enhanced when the temperature increases (Figure S20). To better understand the mechanism of such energy transfer, the lifetimes of the excited states $^5D_0$ (Eu^{3+}) and $^5D_4$ (Tb^{3+}) at different temperature within these luminescent MOFs were monitored at 613 and 545 nm, respectively (Figure S21−S24). The lifetime of $^5D_0$ in **Eu-DMBDC** and $^5D_4$ in **Tb-DMBDC** decrease by approximately 30% as the temperature is increased from 10 to 300 K. However, there is no significant decrease of the $^5D_0$ (Eu^{3+}) lifetime in **$Eu_{0.0069}Tb_{0.9931}$-DMBDC**. The fact that, at the same temperature, **$Eu_{0.0069}Tb_{0.9931}$-DMBDC** exhibits shorter $^5D_4$ (Tb^{3+}) lifetime than **Tb-DMBDC**; while longer $^5D_0$ (Eu^{3+}) lifetime than **Eu-DMBDC**, does indicate that the energy transfer from the Tb^{3+} to Eu^{3+} occurs. In theory, the efficiency of energy transfer (E) between the donor and acceptor can be calculated from the lifetime of donor luminescence:[33]

$$E = 1 - \frac{\tau_{da}}{\tau_d} \quad (2)$$

where τ_{da} and τ_d are the donor's excited-state lifetime in the presence and absence of the acceptor, respectively. The calculated energy transfer efficiency of the Tb^{3+} to Eu^{3+} transition in **$Eu_{0.0069}Tb_{0.9931}$-DMBDC** displays stable enhancement at the elevated temperature (Figure S25). Such energy transfer might be mainly controlled by the phonon-assisted Förster transfer mechanism.[34,35]

In summary, we developed a luminescent mixed lanthanide MOF approach and realized the first MOF thermometer based

dx.doi.org/10.1021/ja2108036 | J. Am. Chem. Soc. 2012, 134, 3979−3982

on two emissions at a wide temperature range which is robust, reliable, and instantaneous. In order to fulfill luminescent Eu^{3+}/Tb^{3+} mixed MOF thermometers, the organic linkers need to have the suitable triplet excited state energy in the range of 22000−24000 cm^{-1} to match the energy of the main accepting level of Eu^{3+} ($^5D_1$, 19030 cm^{-1}) and Tb^{3+}($^5D_4$, 20500 cm^{-1}), thus sensitizing both Eu^{3+} and Tb^{3+} emissions simultaneously and efficiently.[36] On the basis of the time-dependent DFT calculation, the H_2DMBDC has the triplet excited state energy of 23306 cm^{-1} which has enabled it as the efficient organic linker for such a purpose. This luminescent MOF thermometer represents a significant step forward in cryogenic temperature sensors due to the excellent linear correlation between temperature and luminescence intensity ratio from 50 to 200 K. Additionally, the richness of organic linkers to tune their different triplet excited state energy and thus to sensitize different combination of lanthanide ions in their luminescent mixed lanthanide MOFs and to construct diverse MOF structures to optimize the energy transfer among the lanthanide ions has enabled this very promising luminescent mixed lanthanide MOF approach to realize practically useful luminescent thermometers with high sensitivity and a tunable response range. Because we can further explore nanoscale mixed lanthanide MOFs,[37] these new luminescent thermometers can be further applied as nanothermometers in intracellular sensing and thermal mapping with nanospatial resolution in the near future.

■ ASSOCIATED CONTENT

Supporting Information

X-ray structure data in CIF format, experimental procedures and characterization data. This material is available free of charge via the Internet at http://pubs.acs.org.

■ AUTHOR INFORMATION

Corresponding Author

gdqian@zju.edu.cn; banglin.chen@utsa.edu

Notes

The authors declare no competing financial interest.

■ ACKNOWLEDGMENTS

This work was supported by the Award AX-1730 from Welch Foundation (B.C.). We gratefully acknowledge the financial support for this work from the National Natural Science Foundation of China (Nos. 50802084, 50928201, 50972127, and 51010002) and the Fundamental Research Funds for the Central Universities.

■ REFERENCES

(1) Allendorf, M. D.; Bauer, C. A.; Bhakta, R. K.; Houk, R. J. T. *Chem. Soc. Rev.* **2009**, *38*, 1330.

(2) Rocha, J.; Carlos, L. D.; Paz, F. A. A.; Ananias, D. *Chem. Soc. Rev.* **2011**, *40*, 926.

(3) Chen, B.; Xiang, S.; Qian, G. *Acc. Chem. Res.* **2010**, *43*, 1115.

(4) Cui, Y; Yue, Y.; Qian, G; Chen, B. *Chem. Rev.* **2012**, *112*, 1126.

(5) Reineke, T. M.; Eddaoudi, M.; Fehr, M.; Kelley, D.; Yaghi, O. M. *J. Am. Chem. Soc.* **1999**, *121*, 1651.

(6) Kreno, L. E.; Leong, K.; Farha, O. K.; Allendorf, M.; Van Duyne, R. P.; Hupp, J. T. *Chem. Rev.* **2012**, *112*, 1105.

(7) Takashima, Y.; Martínez, V. M.; Furukawa, S.; Kondo, M.; Shimomura, S.; Uehara, H.; Nakahama, M.; Sugimoto, K.; Kitagawa, S. *Nat. Commun.* **2011**, *2*, 168.

(8) Yanai, N.; Kitayama, K.; Hijikata, Y.; Sato, H.; Matsuda, R.; Kubota, Y.; Takata, M.; Mizuno, M.; Uemura, T.; Kitagawa, S. *Nat. Mater.* **2011**, *10*, 787.

(9) White, K. A.; Chengelis, D. A.; Gogick, K. A.; Stehman, J.; Rosi, N. L.; Petoud, S. *J. Am. Chem. Soc.* **2009**, *131*, 18069.

(10) An, J.; Shade, C. M.; Chengelis-Czegan, D. A.; Petoud, S. p.; Rosi, N. L. *J. Am. Chem. Soc.* **2011**, *133*, 1220.

(11) Stylianou, K. C.; Heck, R.; Chong, S. Y.; Bacsa, J.; Jones, J. T. A.; Khimyak, Y. Z.; Bradshaw, D.; Rosseinsky, M. J. *J. Am. Chem. Soc.* **2010**, *132*, 4119.

(12) Rieter, W. J.; Taylor, K. M. L.; Lin, W. *J. Am. Chem. Soc.* **2007**, *129*, 9852.

(13) Xie, Z.; Ma, L.; deKrafft, K. E.; Jin, A.; Lin, W. *J. Am. Chem. Soc.* **2010**, *132*, 922.

(14) Lan, A.; Li, K.; Wu, H.; Olson, D. H.; Emge, T. J.; Ki, W.; Hong, M.; Li, J. *Angew. Chem., Int. Ed.* **2009**, *121*, 2370.

(15) Jiang, H.-L.; Tatsu, Y.; Lu, Z.-H.; Xu, Q. *J. Am. Chem. Soc.* **2010**, *132*, 5586.

(16) Chandler, B. D.; Cramb, D. T.; Shimizu, G. K. H. *J. Am. Chem. Soc.* **2006**, *128*, 10403.

(17) Qi, X.-L.; Lin, R.-B.; Chen, Q.; Lin, J.-B.; Zhang, J.-P.; Chen, X.-M. *Chem. Sci.* **2011**, *2*, 2214.

(18) Shustova, N. B.; McCarthy, B. D.; Dinca, M. *J. Am. Chem. Soc.* **2011**, *133*, 20126.

(19) Harbuzaru, B. V.; Corma, A.; Rey, F.; Atienzar, P.; Jordá, J. L.; García, H.; Ananias, D.; Carlos, L. D.; Rocha, J. *Angew. Chem., Int. Ed.* **2008**, *47*, 1080.

(20) Chen, B.; Wang, L.; Zapata, F.; Qian, G.; Lobkovsky, E. B. *J. Am. Chem. Soc.* **2008**, *130*, 6718.

(21) Chen, B.; Wang, L.; Xiao, Y.; Fronczek, F. R.; Xue, M.; Cui, Y.; Qian, G. *Angew. Chem., Int. Ed.* **2009**, *48*, 500.

(22) Chen, B.; Yang, Y.; Zapata, F.; Lin, G.; Qian, G.; Lobkovsky, E. B. *Adv. Mater.* **2007**, *19*, 1693.

(23) Xiao, Y.; Cui, Y.; Zheng, Q.; Xiang, S.; Qian, G.; Chen, B. *Chem. Commun.* **2010**, *46*, 5503.

(24) Xu, H.; Liu, F.; Cui, Y.; Chen, B.; Qian, G. *Chem. Commun.* **2011**, *47*, 3153.

(25) Binnemans, K. *Chem. Rev.* **2009**, *109*, 4283.

(26) Carlos, L. D.; Ferreira, R. A. S.; de Zea Bermudez, V.; Julián-López, B.; Escribano, P. *Chem. Soc. Rev.* **2011**, *40*, 536.

(27) Brites, C. D. S.; Lima, P. P.; Silva, N. J. O.; Millán, A.; Amaral, V. S.; Palacio, F.; Carlos, L. D. *New J. Chem.* **2011**, *35*, 1177.

(28) Brites, C. D. S.; Lima, P. P.; Silva, N. J. O.; Millán, A.; Amaral, V. S.; Palacio, F.; Carlos, L. D. *Adv. Mater.* **2010**, *22*, 4499.

(29) Peng, H.; Stich, M. I. J.; Yu, J.; Sun, L.-N.; Fischer, L. H.; Wolfbeis, O. S. *Adv. Mater.* **2010**, *22*, 716.

(30) Vetrone, F.; Naccache, R.; Zamarrón, A.; Juarranz de la Fuente, A.; Sanz-Rodríguez, F.; Martinez Maestro, L.; Martín Rodriguez, E.; Jaque, D.; García Solé, J.; Capobianco, J. A. *ACS Nano* **2010**, *4*, 3254.

(31) Sun, L.-N.; Yu, J.; Peng, H.; Zhang, J. Z.; Shi, L.-Y.; Wolfbeis, O. S. *J. Phys. Chem. C* **2010**, *114*, 12642.

(32) Yu, J.; Sun, L.; Peng, H.; Stich, M. I. J. *J. Mater. Chem.* **2010**, *20*, 6975.

(33) Xiao, M.; Selvin, P. R. *J. Am. Chem. Soc.* **2001**, *123*, 7067.

(34) Auzel, F. *Chem. Rev.* **2004**, *104*, 139.

(35) Liu, Y.; Qian, G.; Wang, Z.; Wang, M. *Appl. Phys. Lett.* **2005**, *86*, 071907.

(36) Parker, D. *Coord. Chem. Rev.* **2000**, *205*, 109.

(37) Lin, W.; Rieter, W. J.; Taylor, K. M. L. *Angew. Chem., Int. Ed.* **2009**, *48*, 650.